Radboud University Nijmegen

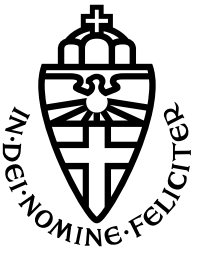


Institute for Mathematics, Astrophysics and Particle Physics
Department of High Energy Physics

# Photon-Baryon Fluid Physics in a Curvature Dependent Dark Energy Universe

Making a prediction on the cosmic microwave background power spectrum in a universe with a dynamical dark energy

Thesis BSc Physics and Astronomy
November 2023

*Author:*
Tijmen Melssen

*Supervisor:*
Prof. Dr. W.J.P. Beenakker

*Second reader:*
Dr. B.P. Bonga

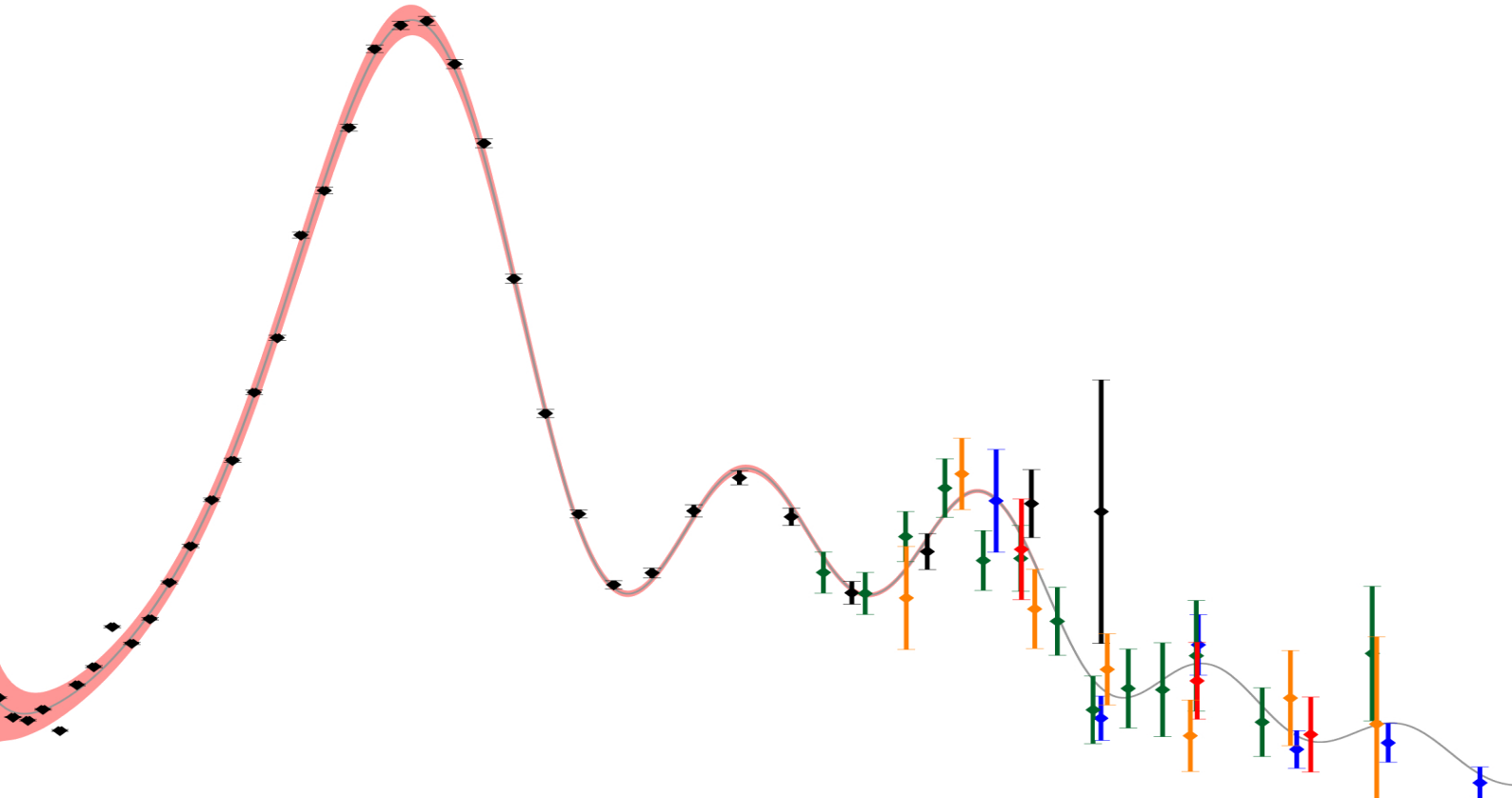

# Acknowledgements

I would like to thank everyone who played a pivotal role in the completion of my thesis. First and foremost, I want to thank my supervisor, Wim Beenakker, for his guidance over the last six months. His mindset of not taking others' assumptions for granted taught me a lot about critical thinking. I enjoyed our weekly meetings, where Wim provided us with good feedback, especially when we were in tears because things did not work out as planned.
I would also like to thank my fellow students, Bas van den Hoek, Thijs van Rossum and Jesse Cools, who worked on the CDDE project alongside me. I enjoyed our collaboration and discussions, not only about physics but also about random YouTube videos and other philosophical discussions near the coffee counter.
Last but not least, I want to thank those who were not mentioned by name but still supported me. Their small gestures of help were incredibly helpful in the end.

*The image on the cover is the cosmic microwave background power spectrum. It is a graphical representation of the amplitude of the temperature fluctuations at different spatial scales. This image is an edited version of the power spectrum in [1].*

# Contents

# 1 Introduction

Cosmology is the field of physics that investigates the origin, structure and evolution of the observable universe on the largest scales. It delves into fundamental questions about the universe: What happened at the big bang? Why do we have structure formation (like galaxies) instead of a homogeneous distribution of matter and energy? What is the future of the universe? What information can we extract from the cosmic microwave background? This last question is what we are going to explore in this thesis. We are researching an alternative cosmological model to investigate its implications on the interpretation of the cosmic microwave background power spectrum.
The main reason to test for alternative cosmological models is the Hubble tension introduced in the $\Lambda$ - cold dark matter model ($\Lambda$-CDM), which is seen as the standard model of Big Bang cosmology. The Hubble tension could hint at flaws within this model. The alternative model we are going to explore uses a curvature dependent dark energy (CDDE) instead of the cosmological constant used in $\Lambda$-CDM. Our CDDE model can indeed solve the Hubble tension, as confirmed by the work of Bas van den Hoek [2] and Thijs van Rossum [3] in their theses .
Another result in the CDDE model is that non-relativistic matter and dark energy are coupled in the evolution equations, resulting in the creation of matter while the universe expands. We hope that this creation of matter could be explained as the source of dark matter, therefore we will not be using any other dark matter sources in this thesis.
In the first few chapters we will delve into the main theory of cosmology, namely the Einstein field equations and necessary assumptions about the universe. We will derive some equations for the CDDE model from the Einstein field equations and compare them to the equations in $\Lambda$-CDM. After that we will look into the physics of the photon-baryon fluid, that is the hot dense plasma present in the early universe. We investigate the relevant approximations and deduce an equation for the speed of sound in this plasma. The speed of sound makes it possible to calculate the sound horizon, which is the maximum distance a sound wave could have travelled in the plasma. We will also look at the anisotropies of the temperature of the cosmic microwave background. These anisotropies can be plotted in a power spectrum, which is comparable to how Fourier series decompose functions into sinusoidal components. We will calculate the expected location of the first peak in the power spectrum for the CDDE model, including the correction due to driving effects. These driving effects are mainly the Doppler shift due to the oscillation of the fluid and the decay of the gravitational potential. The sound horizon and the first peak's multipole moment are seen as standard candles in cosmology, so they provide a good comparison with the observations done by astrophysicists.

# 2 Conventions

## Units

In this thesis we make use of the natural units, where

$$c = \hbar = k_{\mathrm{B}} = \mu_0 = \epsilon_0 = 1$$

by absorbing these constants in the relevant fields and quantities. This leads to the following relation between the units of key quantities

$$[\text{energy}] = [\text{mass}] = [\text{length}]^{-1} = [\text{time}]^{-1}.$$

## Tensors

Greek indices are used for spacetime coordinates $(t, x, y, z)$ or $(x^0, x^1, x^2, x^3)$. Latin indices are used for the spatial dimensions.
We also make use of the Einstein summation convention, where we sum over repeated indices. This means that

$$c_\mu x^\mu = \sum_\mu c_\mu x^\mu = c_0 x^0 + c_1 x^1 + c_2 x^2 + c_3 x^3.$$

Note: the sum must contain an upper and a lower index.
Raising and lowering indices can be done with the metric

$$c_\mu = g_{\mu\nu} c^\nu.$$

The metric has the so-called "mostly minus" signature.

## Other Practicalities

When using logarithms, "log" represents the natural logarithm.
Subscripts used in the scale factor, redshift values etc. often denote moments in time. The subscript 0 denotes the present time value. For example: $T_0$ is the temperature at present time, $a_0$ is the scale factor at present time etc.
Furthermore we use Newton's dot notation for differentiation with respect to time:

$$\dot{y} = \frac{\mathrm{d}y}{\mathrm{d}t}, \quad \ddot{y} = \frac{\mathrm{d}^2 y}{\mathrm{d}t^2}.$$

# 3 The Basics of Cosmology

## 3.1 Einstein Field Equations and FRW Metric

One of the main pillars of cosmology is general relativity, as formulated by Einstein in 1915. General relativity provides the theoretical framework for understanding the large-scale structure and dynamics of the universe. The basis for this theory are the Einstein field equations, which relate the curvature of spacetime to the energy, momentum and stress within that spacetime. The equations are given by

$$R_{\mu\nu} - \frac{1}{2} g_{\mu\nu} R = 8\pi G T^{\text{eff}}_{\mu\nu}, \tag{3.1}$$

where $R_{\mu\nu}$ and $R$ are the Ricci tensor and scalar, $g_{\mu\nu}$ is the metric, $G$ is the gravitational constant and $T^{\text{eff}}_{\mu\nu}$ is the effective (total) stress-energy tensor.
From here we have to make some assumptions about the universe. The first one is that the universe is isotropic and homogeneous on scales larger than roughly 100 Mpc [4, 5]. Isotropic means that there is no preferred direction and homogeneous means that there is no preferred location in the universe, see figure 1. So the universe will look the same in all directions and at all locations beyond distances of roughly 100 Mpc.

Figure 1: Left: an anisotropic, but homogeneous pattern on scales much larger than the stripe width. Right: an isotropic about the origin, but inhomogeneous pattern [4].

Treating the universe as isotropic and homogeneous is called the cosmological principle or the perfect fluid approximation, which allows us to use the Friedmann-Robertson-Walker metric (FRW metric). This metric describes the geometry of the universe. In spherical coordinates $(t, r, \theta, \phi)$, the FRW metric is given by

$$g^{\text{FRW}}_{\mu\nu} = \text{diag}\left(1, -\frac{a^2(t)}{1-\kappa r^2}, -a^2(t) r^2, -a^2(t) r^2 \sin^2(\theta)\right), \tag{3.2}$$

where $a(t)$ is the scale factor and $\kappa$ describes the intrinsic spatial curvature of the universe. The scale factor relates the proper distance, which can change over time, between two objects moving in an expanding or contracting FRW universe according to

$$d(t) = a(t) d_0, \tag{3.3}$$

here $d(t)$ is the proper distance at time $t$ and $d_0$ is the proper distance at a reference time $t_0$. Thus $d_0 = d(t_0)$ and $a(t_0) = 1$.
The intrinsic curvature $\kappa$ of the universe is described by its spatial curvature. Spatial curvature determines if the universe is positively curved (spherical, $\kappa > 0$), negatively curved (hyperbolic, $\kappa < 0$) or flat ($\kappa = 0$). This is depicted in figure 2.

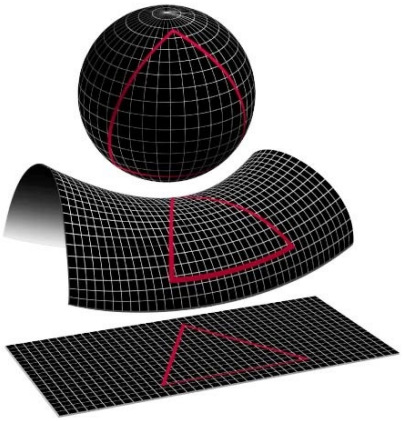

Figure 2: The three spatial curvatures for the universe, from top to bottom: positively curved (spherical), negatively curved (hyperbolic) and flat [6].

The second assumption we make is that the universe is flat, so there is no intrinsic curvature (i.e. $\kappa = 0$). This is one of the high certainty measurements that follow from the Λ-CDM model [1] (see section 4), and which we will assume to be true in general. The FRW metric then reduces to

$$g_{\mu\nu}^{\text{FRW}} = \text{diag}\left(1, -a^2(t), -a^2(t)r^2, -a^2(t)r^2\sin^2(\theta)\right). \tag{3.4}$$

Another useful concept is redshift. Redshift is the increase in wavelength of electromagnetic radiation due to the expansion of the universe. The redshift $z$ is related to the scale factor as

$$1 + z = \frac{1}{a}. \tag{3.5}$$

In cosmology it makes more sense to use redshift as a time coordinate rather than time itself. This is because redshift is a measurable quantity, while time is relative and can be affected by factors such as the motion of the observer and gravitational fields. A redshift of 0 corresponds to the present time and a redshift greater than 0 corresponds to the past.

## 3.2 Ricci Tensor and Scalar

The Ricci tensor and scalar, which are necessary to solve equation (3.1), can be deduced from the FRW metric (3.4). We can do this by first calculating the Christoffel symbols

$$\Gamma^{\mu}_{\nu\rho} = \frac{1}{2}g^{\mu\sigma}\left(\partial_\nu g_{\sigma\rho} + \partial_\rho g_{\nu\sigma} - \partial_\sigma g_{\nu\rho}\right), \tag{3.6}$$

where $g^{\mu\sigma}$ is the inverse (FRW) metric and $\partial_\nu \equiv \partial/\partial x^\nu$. The non-zero Christoffel symbols are

$$\begin{aligned}
&\Gamma^t_{rr} = a\dot{a} && \Gamma^t_{\theta\theta} = r^2 a\dot{a} && \Gamma^t_{\phi\phi} = r^2\sin^2(\theta)a\dot{a} \\
&\Gamma^r_{tr} = \Gamma^\theta_{t\theta} = \Gamma^\phi_{t\phi} = \frac{\dot{a}}{a} && \Gamma^r_{\theta\theta} = -r && \Gamma^r_{\phi\phi} = -r\sin^2(\theta) \\
&\Gamma^\theta_{r\theta} = \frac{1}{r} && \Gamma^\theta_{\phi\phi} = -\cos(\theta)\sin(\theta) && \\
&\Gamma^\phi_{r\phi} = \frac{1}{r} && \Gamma^\phi_{\phi\theta} = \cot(\theta) &&
\end{aligned} \tag{3.7}$$

which are all symmetric in the lower two indices. The Christoffel symbols can be used to calculate the Riemann curvature tensor

$$R^{\sigma}_{\mu\nu\rho} = \partial_\nu \Gamma^{\sigma}_{\mu\rho} - \partial_\rho \Gamma^{\sigma}_{\mu\nu} + \Gamma^{\alpha}_{\mu\rho}\Gamma^{\sigma}_{\alpha\nu} - \Gamma^{\alpha}_{\mu\nu}\Gamma^{\sigma}_{\alpha\rho}. \tag{3.8}$$

The Ricci tensor and scalar are given by

$$R_{\mu\rho} = R^{\nu}_{\mu\nu\rho} \tag{3.9}$$

$$R = g^{\mu\rho} R_{\mu\rho}, \tag{3.10}$$

resulting in

$$R_{00} = -3\frac{\ddot{a}}{a} \tag{3.11}$$

$$R_{kk} = -\left(\frac{\ddot{a}}{a} + 2\frac{\dot{a}^2}{a^2}\right) g^{\mathrm{FRW}}_{kk} \tag{3.12}$$

$$R_{\mu\nu} = 0 \qquad \text{if } \mu \neq \nu \tag{3.13}$$

$$R = -6\left(\frac{\ddot{a}}{a} + \frac{\dot{a}^2}{a^2}\right). \tag{3.14}$$

## 3.3 Stress-Energy Tensors

The only tensor left to be specified in order to be able to solve equation (3.1) is the effective stress-energy tensor $T^{\mathrm{eff}}_{\mu\nu}$. For our assumptions the stress-energy tensors are diagonal. The $T_{00}$ component represents the energy density and the $T_{kk}$ components represent the pressure in the $k$-th spatial direction.
For relativistic and non-relativistic matter, the stress-energy tensor is given by

$$T^{\mathrm{mat}}_{\mu\nu} = \mathrm{diag}\left(\rho, -p g^{\mathrm{FRW}}_{11}, -p g^{\mathrm{FRW}}_{22}, -p g^{\mathrm{FRW}}_{33}\right), \tag{3.15}$$

where $\rho = \rho_{\mathrm{r}} + \rho_{\mathrm{m}}$ represents the energy density of the fluid and $p = p_{\mathrm{r}} + p_{\mathrm{m}}$ denotes the pressure term. We use the subscript 'r' to indicate relativistic particles (radiation) and the subscript 'm' to indicate non-relativistic particles (matter). For radiation, the pressure term is given by $p_{\mathrm{r}} = \frac{1}{3}\rho_{\mathrm{r}}$, while for matter, it is $p_{\mathrm{m}} = 0$, as discussed in subsection 6.3. It is important to note that throughout this thesis, the symbols $\rho$ and $p$ will consistently represent the density and pressure for both radiation and matter.
According to quantum field theory, empty space (in the absence of matter and radiation) is not truly empty but contains a background energy, called the vacuum energy or dark energy. This vacuum energy, denoted by the stress-energy tensor $T^{\mathrm{vac}}_{\mu\nu}$, has observable effects, such as a contribution to the expansion of the universe. However, the origin is still unknown and has sparked various speculations. We will discuss the main cosmological model implementing the vacuum energy, known as the $\Lambda$ - cold dark matter model, in the next section.

# 4 $\Lambda$ - Cold Dark Matter Model

The $\Lambda$ - cold dark matter model ($\Lambda$-CDM) is often seen as the standard model of Big Bang cosmology, it is one of the simplest models that successfully explains a wide range of observations, i.e. the large-scale structure of the universe and the cosmic microwave background radiation (CMB). In this model the vacuum energy is taken as a constant, called the cosmological constant $\Lambda$. In the $\Lambda$-CDM model the Einstein field equations are often given as

$$R_{\mu\nu} - \frac{1}{2}g_{\mu\nu}R - \Lambda g_{\mu\nu} = 8\pi G T^{\text{mat}}_{\mu\nu}. \tag{4.1}$$

This equation can easily be rewritten in the form of equation (3.1) if we take the effective stress-energy tensor as

$$T^{\text{eff}}_{\mu\nu} = T^{\text{mat}}_{\mu\nu} + \frac{\Lambda}{8\pi G}g_{\mu\nu}. \tag{4.2}$$

In this model the vacuum stress-energy tensor is thus

$$T^{\text{vac}}_{\mu\nu} = \frac{\Lambda}{8\pi G}g_{\mu\nu}, \tag{4.3}$$

which is constant under the expansion of the universe.
A few results following from the $\Lambda$-CDM model are

$$\dot{\rho_{\text{m}}} + \dot{\rho_{\text{r}}} + \frac{\dot{a}}{a}\left(3\rho_{\text{m}} + 4\rho_{\text{r}}\right) = 0, \tag{4.4}$$

$$\frac{\dot{a}^2}{a^2} = \frac{8\pi G}{3}\left(\rho_{\text{m}} + \rho_{\text{r}} + \frac{\Lambda}{8\pi G}\right) \quad \Rightarrow \quad \bar{\Omega} \equiv 1 = \Omega_{\text{m}} + \Omega_{\text{r}} + \Omega_{\Lambda}, \tag{4.5}$$

where $\Omega_{\text{m}} \equiv \frac{8\pi G}{3H^2}\rho_{\text{m}}$, $\Omega_{\text{r}} \equiv \frac{8\pi G}{3H^2}\rho_{\text{r}}$, $\Omega_{\Lambda} \equiv \frac{\Lambda}{3H^2}$ and $H(t) \equiv \frac{\dot{a}}{a}$. The quantity denoted as $H(t)$ is called the Hubble parameter, describing the expansion rate of the universe at a given time $t$. The $\Omega_i$-terms are dimensionless density parameters, enabling us to get a nice boundary condition for their sum. The Hubble parameter at present time is called the Hubble constant and is denoted as $H_0$.
In this model it is assumed that matter and radiation do not interact with each other. This is a good assumption for the late universe, but not necessarily for the time period when the universe consisted of a hot photon-baryon fluid. We will delve deeper into this epoch in section 6. This assumption makes it possible to split equation (4.4) into two equations, making it possible to solve the system of equations for $a$, $\rho_{\text{m}}$ and $\rho_{\text{r}}$. This results in the relation between energy densities, scale factor and redshift as [4]

$$\rho_{\text{m}} = \rho_{\text{m},0}a^{-3} = \rho_{\text{m},0}(1+z)^3 \tag{4.6}$$

$$\rho_{\text{r}} = \rho_{\text{r},0}a^{-4} = \rho_{\text{r},0}(1+z)^4. \tag{4.7}$$

## 4.1 Hubble Tension

The $\Lambda$-CDM model can explain various observations, including the cosmic microwave background radiation, large-scale structure formation and baryonic acoustic oscillations, among others. However, this does not imply that the model is flawless. In fact, it introduces the Hubble tension. The tension arises from the fact that there are two main methods to determine the Hubble constant $H_0$ [7].
The first method is the observation of redshift (to determine the recession velocity) and the distance of relatively nearby galaxies; therefore, these measurements are referred to as local measurements. This method is cosmological model independent, because these are direct measurements from the universe close to the present time. The current value

for this late universe measurement is $H_0^{\text{late}} = 73.3 \pm 0.8\,\text{km/s/Mpc}$ [7].
The second method is the study of tiny temperature fluctuations in the cosmic microwave background (CMB) radiation, which we will discuss in section 7. This method is cosmological model dependent, because the evolution of the universe influences the interpretation of the data that originates from the early universe. The current value of this early universe measurement is $H_0^{\text{early}} = 67.4 \pm 0.5\,\text{km/s/Mpc}$ [7].
Both methods result in different values for the Hubble constant, as shown in figure 3. This difference is called the Hubble tension.

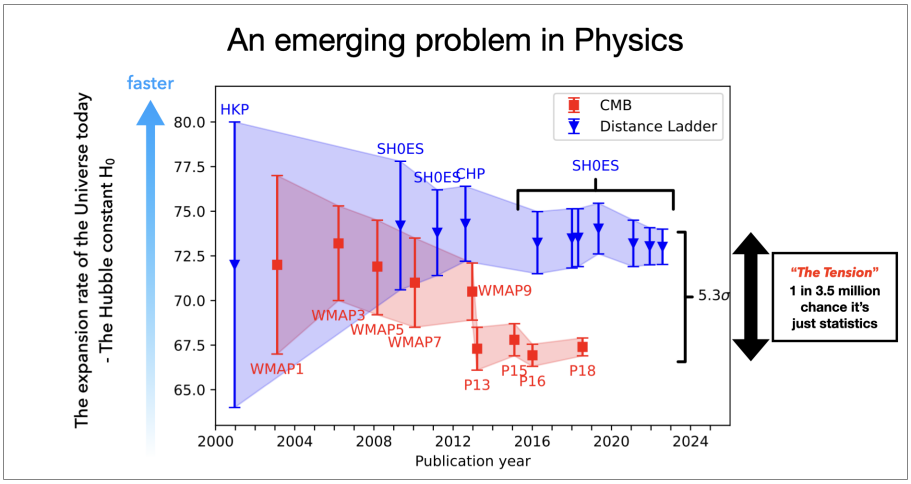


Figure 3: A variety of measurements of the Hubble constant $H_0$ [8]. The blue data points are the local measurements and the red data points are the cosmic microwave background measurements. The dimension of $H_0$ on the $y$-axis is [km/s/Mpc]. It is clearly visible that two different values are obtained in the $\Lambda$-CDM model.

The Hubble tension prompted Prof. Dr. W.J.P. Beenakker to explore possible solutions to alleviate this tension. In collaboration with David Venhoek, as presented in their paper [9], it is shown that two possible ways to solve the tension are:

- A dark energy term which is not a constant over time/redshift.
- Matter that does not evolve according to the conventional $\rho_{\text{m}} \propto a^{-3}$ dependence.

These two approaches can be implemented into a new cosmological model, which we will investigate in this thesis.

# 5 Curvature Dependent Dark Energy Model

## 5.1 Solving the Einstein Equations

It is interesting to investigate what happens when we introduce a stress-energy tensor dependent on the scalar curvature of spacetime for the vacuum energy. In general, this tensor can be written as

$$T_{\mu\nu}^{\text{vac}} = C_\gamma \left(-\frac{R}{6}\right)^\gamma g_{\mu\nu}^{\text{FRW}} \tag{5.1}$$

where $C_\gamma$ is a dimensionful constant for arbitrary $\gamma$ and $R$ is the Ricci scalar. Here we divide by 6 to eliminate the prefactor in the Ricci scalar (3.14). The effective stress-energy tensor is simply the sum of both tensors, resulting in

$$T_{\mu\nu}^{\text{eff}} = T_{\mu\nu}^{\text{mat}} + T_{\mu\nu}^{\text{vac}} = \text{diag}\left(\rho, -pg_{11}^{\text{FRW}}, -pg_{22}^{\text{FRW}}, -pg_{33}^{\text{FRW}}\right) + C_\gamma \left(-\frac{R}{6}\right)^\gamma g_{\mu\nu}^{\text{FRW}}. \tag{5.2}$$

The $\mu = \nu = 0$ component of equation (3.1) leads to

$$\frac{\dot{a}^2}{a^2} = \frac{8\pi G}{3}\left(\rho + C_\gamma \left(\frac{\ddot{a}}{a} + \frac{\dot{a}^2}{a^2}\right)^\gamma\right), \tag{5.3}$$

The $\mu = \nu \neq 0$ components can be calculated and simplified (by eliminating the vacuum energy term) by substitution of equation (5.3), this leads to an acceleration equation

$$\frac{\ddot{a}}{a} = \frac{\dot{a}^2}{a^2} - 4\pi G(\rho + p). \tag{5.4}$$

These equations are variations on the Friedmann equations in our model universe. They are useful because they link together the scale factor $a$, the total energy density and the rate at which the scale factor changes over time.

## 5.2 Special Case: $\gamma = \frac{1}{2}$

Equation (5.4) leads to the $\Lambda$-CDM model for $\gamma = 0$, but it is interesting to check what happens for a different $\gamma$ value. The unit of the Ricci scalar is $[R] = \frac{1}{L^2} \sim \text{GeV}^2$, thus the square root of the Ricci scalar results in the lowest possible (integer) value of energy units. So an educated guess would be to check the special case $\gamma = 1/2$, which we will call the curvature dependent dark energy universe (CDDE). The stress-energy tensor for the vacuum energy then becomes

$$T_{\mu\nu}^{\text{vac}} = C_{1/2}\left(-\frac{R}{6}\right)^{1/2} g_{\mu\nu}^{\text{FRW}}, \tag{5.5}$$

which implies that the vacuum energy is not constant during the evolution of the universe. This is the first of the two conditions mentioned in section 4 to be able to solve the Hubble tension. The effective stress-energy tensor now reads

$$T_{\mu\nu}^{\text{eff}} = \text{diag}\left(\rho, -pg_{11}^{\text{FRW}}, -pg_{22}^{\text{FRW}}, -pg_{33}^{\text{FRW}}\right) + C_{1/2}\left(-\frac{R}{6}\right)^{1/2} g_{\mu\nu}^{\text{FRW}}. \tag{5.6}$$

As a result equation (5.3) becomes

$$\frac{\dot{a}^2}{a^2} = \frac{8\pi G}{3}\left(\rho + C_{1/2}\left(\frac{\ddot{a}}{a} + \frac{\dot{a}^2}{a^2}\right)^{1/2}\right). \tag{5.7}$$

Combining equations (5.4) and (5.7) leads to

$$\frac{\ddot{a}}{a} = -\frac{4\pi G}{3}\left(\rho + 3p - \beta \pm \sqrt{\beta(\rho - 3p + \beta)}\right), \tag{5.8}$$

where we have defined $\beta \equiv \frac{16\pi G}{3} C_{1/2}^2$ to clean up the equation. To check whether the $\pm$ sign should be positive or negative, we can use that

$$\frac{\ddot{a}}{a} + \frac{4\pi G}{3}(\rho + 3p) = -\frac{4\pi G}{3}\left(-\beta \pm \sqrt{\beta(\rho - 3p + \beta)}\right) \geq 0 \tag{5.9}$$

for $C_{1/2} > 0$, as required for obtaining the positively accelerating universe we presently live in [10]. The minus sign is therefore the correct one, resulting in a second acceleration equation independent of $\dot{a}$

$$\frac{\ddot{a}}{a} = -\frac{4\pi G}{3}\left(\rho + 3p - \beta - \sqrt{\beta(\rho - 3p + \beta)}\right). \tag{5.10}$$

Combining equations (5.4) and (5.10) and differentiating with respect to time we find

$$\dot{\rho}_{\mathrm{m}} + \dot{\rho}_{\mathrm{r}} + \frac{\sqrt{\beta}}{4\sqrt{\rho_{\mathrm{m}} + \beta}}\dot{\rho}_{\mathrm{m}} + \frac{\dot{a}}{a}\left(3\rho_{\mathrm{m}} + 4\rho_{\mathrm{r}}\right) = 0. \tag{5.11}$$

The combination of equations (5.4) and (5.10) can also be rearranged to

$$\overline{\Omega} \equiv 1 = \Omega_{\mathrm{m}} + \Omega_{\mathrm{r}} + \frac{1}{2}\Omega_\beta\left(1 + \sqrt{\frac{\Omega_{\mathrm{m}}}{\Omega_\beta} + 1}\right), \tag{5.12}$$

where $\Omega_{\mathrm{m}} \equiv \frac{8\pi G}{3H^2}\rho_{\mathrm{m}}$, $\Omega_{\mathrm{r}} \equiv \frac{8\pi G}{3H^2}\rho_{\mathrm{r}}$, $\Omega_\beta \equiv \frac{8\pi G}{3H^2}\beta$ and $H \equiv \frac{\dot{a}}{a}$. It can be immediately seen that these equations are fundamentally different from equations (4.4) and (4.5) in the $\Lambda$-CDM model. These equations are useful because they describe the evolution of $\rho_{\mathrm{m}}$ and $\rho_{\mathrm{r}}$ over time. They also give constraints on the values that $\Omega_{\mathrm{m}}$, $\Omega_{\mathrm{r}}$ and $\Omega_\beta$ can take.

## 5.3 Benchmark Model

So far we have obtained two equations describing the evolution of the matter- and radiation density and the scale factor,

$$\dot{\rho}_{\mathrm{m}} + \dot{\rho}_{\mathrm{r}} + \frac{\sqrt{\beta}}{4\sqrt{\rho_{\mathrm{m}} + \beta}}\dot{\rho}_{\mathrm{m}} + \frac{\dot{a}}{a}\left(3\rho_{\mathrm{m}} + 4\rho_{\mathrm{r}}\right) = 0 \tag{5.13}$$

$$\overline{\Omega} \equiv 1 = \Omega_{\mathrm{m}} + \Omega_{\mathrm{r}} + \frac{1}{2}\Omega_\beta\left(1 + \sqrt{\frac{\Omega_{\mathrm{m}}}{\Omega_\beta} + 1}\right). \tag{5.14}$$

The problem we now stumble upon is that we want to solve these equations for $\rho_{\mathrm{m}}$, $\rho_{\mathrm{r}}$ and $a$. The value for $\beta$ is a parameter that follows from a fit, solving the Hubble tension. These fits were obtained by Bas van den Hoek [2] and Thijs van Rossum [3] in their theses as part of the CDDE project. This leaves us with 3 unknown variables and 2 equations. To be able to solve this system we need one more equation.
In the late universe we live in today, radiation and matter do not interact with each other. In this epoch equation (5.13) can be separated into two equations, one containing $\rho_{\mathrm{m}}$ and the other $\rho_{\mathrm{r}}$, enabling us to solve this system of equations.
In this thesis we will look at the early universe, consisting of a hot photon-baryon plasma. In this plasma there is a lot of interaction between photons and matter (in the form of Thomson scattering) and equation (5.13) cannot be separated that trivially. Here another equation is necessary to solve the system, which we will deduce in subsection 6.1.

## 5.4 Matter Creation

When separating equation (5.13), which we are allowed to do for the late universe, we can solve the system of equations and obtain

$$\rho_{\mathrm{r}} = \rho_{\mathrm{r},0} a^{-4} \tag{5.15}$$

$$\log(\rho_{\mathrm{m}}) + \frac{1}{4}\log\left(\frac{-1+\sqrt{\frac{\rho_{\mathrm{m}}+\beta}{\beta}}}{1+\sqrt{\frac{\rho_{\mathrm{m}}+\beta}{\beta}}}\right) = -3\log(a) + \text{constant}, \tag{5.16}$$

where the constant is determined by $\rho_{\mathrm{m},0}$ [2]. These equations clearly show that matter and dark energy are coupled. Equation (5.16) can be written in the form

$$\rho_{\mathrm{m}} = \rho_{\mathrm{m},0} a^{-B}, \tag{5.17}$$

where $B$ is variable for different values of redshift [2]. Notice how equation (5.17) is not equal to (4.6) for $B \neq 3$. This is due to the creation of matter caused by the change in vacuum energy. The values for $B$ for different redshifts are plotted in figure 4.

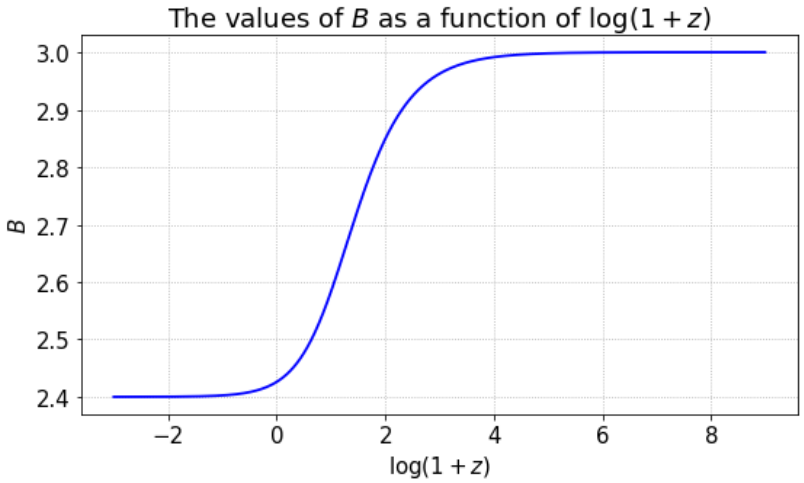


Figure 4: Plot of the values of $B$ in $\rho_{\mathrm{m}} = \rho_{\mathrm{m},0} a^{-B}$ as a function of redshift $z$. The redshift is plotted as $\log(1+z)$ since this results in a clearer picture of the cosmological timeline.

From this figure we can deduce that in the early universe the vacuum energy provides a negligible contribution to the creation of matter, resulting in the same energy density formula as found in the $\Lambda$-CDM model

$$\rho_{\mathrm{m}} = \rho_{\mathrm{m},0} a^{-3}. \tag{5.18}$$

For lower values of $z$ the vacuum energy becomes more present and matter is created, such that equation 5.17 asymptotically becomes

$$\rho_{\mathrm{m}} = \rho_{\mathrm{m},0} a^{-2.4}. \tag{5.19}$$

So a cosmological model of this kind also has the second condition in section 4 implemented.
We assume the created matter to be light (Standard Model) neutrinos, since these are

the easiest massive matter particles to create. Dark energy does not couple to radiation, so there is no creation of radiation. Fortunately this is not the case, otherwise this would dissipate the black-body CMB spectrum, which we will come back to in section 7.
In the epoch where matter creation does play a significant role, the energy scale of the dark energy density is not high enough to create massive particles other than neutrinos. We hope that this creation of weakly interacting matter could explain dark matter and that a universe with this cosmological model is feasible without the necessity of other dark matter sources. This means that the energy density of baryonic matter still evolves as

$$\rho_{\mathrm{b}} = \rho_{\mathrm{b},0} a^{-3}. \tag{5.20}$$

The reason to stress this will become clear later on.

# 6 Photon-Baryon Fluid Dynamics

A long time ago the universe consisted of a hot plasma of photons and baryons. In cosmological terms, baryons are the matter components that interact with photons, so the term baryon does also refer to the electrons in the plasma. These electrons are needed for having a plasma that has no net charge. The baryons forming the photon-baryon fluid are created during Big Bang nucleosynthesis, which is the epoch of the production of nuclei other than hydrogen-1. This happened around $z_{\text{nuc}} \approx 2.79 \cdot 10^8$, see also subsection 6.7.
As the universe expanded, it gradually cooled down. When the universe reached a low enough temperature, protons, heavier ions and electrons were able to combine, forming neutral atoms [11]. This transition of a photon-baryon fluid to a gas of neutral atoms is known as recombination. The end of recombination is called the moment of last scattering. This is the moment where photons could scatter on free electrons for the last time. Last scattering happened at a redshift $z = 1270$, see subsection 6.6. This moment is important, because it marks the moment the universe became transparent to radiation.
Prior to recombination, the universe was opaque due to the Thomson scattering of photons by free electrons. However, after recombination, photons could travel freely. These moments are represented in the timeline in figure 5. The photons originating from the photon-baryon fluid are still observable and are referred to as the cosmic microwave background (CMB) [4], a topic we will delve into further in section 7. In the present section we will investigate the physics involved in the dynamics of the photon-baryon fluid.

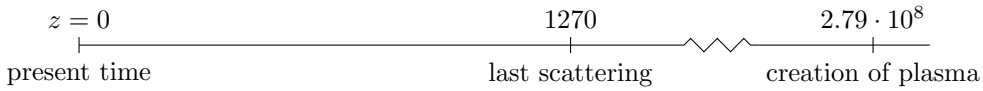


Figure 5: Timeline of the universe, where important moments and their corresponding redshift values are marked.

## 6.1 Black Body Approximation

The cosmic microwave background spectrum closely approximates a perfect black body [12], this implies a thermal equilibrium of the baryons, electrons and photons at the moment of recombination [13]. Since the number of photons is large enough to ionize the atoms in the fluid, it is valid to assume that the photon-baryon fluid was also in thermal equilibrium before recombination. The photons can therefore be described by a black body photon gas [14]. In a black body photon gas, the relation between the average photon energy $\bar{E}_\gamma$, its average wavelength $\bar{\lambda}$ and the gas' temperature $T$ is given by

$$\bar{E}_\gamma = \frac{2\pi}{\bar{\lambda}} = 2.70T. \tag{6.1}$$

The mean photon wavelength expressed in terms of the temperature of the gas is then

$$\bar{\lambda} = \frac{2.33}{T}. \tag{6.2}$$

Redshift can be expressed in terms of the emitted and observed wavelengths [15]

$$z = \frac{\bar{\lambda}_{\text{observed}} - \bar{\lambda}_{\text{emitted}}}{\bar{\lambda}_{\text{emitted}}}. \tag{6.3}$$

It is now possible to deduce an expression for the redshift as function of the temperature by substituting (6.2), this becomes

$$z + 1 = \frac{T_{\text{emitted}}}{T_{\text{observed}}}. \tag{6.4}$$

Now we have a relation between the redshift (and, consequently, the scale factor) and the temperature

$$T = T_0(z + 1) = T_0 a^{-1}, \tag{6.5}$$

where $T_0$ is the observed temperature at the present time, denoted with the subscript 0. This means that the temperature is proportional to the scale factor as

$$T \propto a^{-1}. \tag{6.6}$$

The Stefan-Boltzmann law for the black body radiation energy density [15] is

$$\rho_{\text{r}} = 4\sigma T^4, \tag{6.7}$$

where $\sigma$ is the Stefan-Boltzmann constant. The energy density - scale factor dependence then follows as

$$\rho_r \propto T^4 \quad \Rightarrow \quad \rho_{\text{r}} \propto a^{-4}, \tag{6.8}$$

by substituting equation (6.6). We have now found the third equation necessary to solve the system of equations in our benchmark model in subsection 5.3. It is now clear that equation (5.13) can also be split in the photon-baryon fluid epoch, resulting in the same equations we got for the late universe:

$$\rho_{\text{r}} = \rho_{\text{r},0} a^{-4} \tag{6.9}$$

$$\log(\rho_{\text{m}}) + \frac{1}{4}\log\left(\frac{-1 + \sqrt{\frac{\rho_{\text{m}}+\beta}{\beta}}}{1 + \sqrt{\frac{\rho_{\text{m}}+\beta}{\beta}}}\right) = -3\log(a) + \text{constant}. \tag{6.10}$$

## 6.2 Fluid Components

It is now useful to take a closer look at the composition of $\rho_{\text{r}}$ and $\rho_{\text{m}}$, the reason for this will become clear in the next few subsections. The radiation energy density is the sum of the energy densities of the photons and the so-called cosmic neutrino background (C$\nu$B) neutrinos, which are relativistic during the plasma phase of the universe. These neutrinos are only weakly interacting and are therefore decoupled from the rest of the components of the universe a long time before the photon-baryon fluid epoch [4]. We can write the radiation energy density as

$$\rho_{\text{r}} = \rho_\gamma + \rho_\nu, \tag{6.11}$$

where the subscript $\gamma$ denotes photons and $\nu$ the C$\nu$B neutrinos. In the epochs when the photon energy density is not negligible, the photon energy density can be approximated as the energy density of the CMB photons [4], which are the same photons present in the plasma. Since the CMB spectrum approximates a perfect black body, we can calculate the (CMB) photon energy density at the present time [15] as

$$\rho_{\gamma,0} = 4\sigma T_0^4, \tag{6.12}$$

where $\sigma$ is the Stefan-Boltzmann constant and $T_0$ is the CMB temperature at the present time, which we will discuss in section 7. To calculate the photon energy density at a given redshift, we can substitute equation (6.12) into equation (6.9) and find

$$\rho_\gamma = 4\sigma T_0^4 a^{-4} = 4\sigma T_0^4 (1 + z)^4. \tag{6.13}$$

The neutrino-to-photon energy density ratio [12] is given by

$$\frac{\rho_\nu}{\rho_\gamma} = \frac{7}{8} N_{\text{eff}} \left(\frac{4}{11}\right)^{4/3}, \tag{6.14}$$

where $N_{\text{eff}} = 3.044$ is the effective number of neutrino species. This equation is based on Λ-CDM, but since it is based on physics before Big Bang nucleosynthesis, which happened at $z \approx 3 \cdot 10^8$, we can assume this to be a good approximation (see subsection 6.7). The total radiation energy density is thus

$$\rho_{\text{r}} = \rho_\gamma \left(1 + \frac{7}{8} N_{\text{eff}} \left(\frac{4}{11}\right)^{4/3}\right) \tag{6.15}$$

$$= 4\sigma T_0^4 (1+z)^4 \left(1 + \frac{7}{8} N_{\text{eff}} \left(\frac{4}{11}\right)^{4/3}\right), \tag{6.16}$$

where we have substituted equation (6.13).
Matter consists of baryonic matter and created matter, as explained in subsection 5.4. So the energy density of matter can be written as the sum of baryonic and created dark matter, respectively

$$\rho_{\text{m}} = \rho_{\text{b}} + \rho_{\text{created}}. \tag{6.17}$$

Since the creation of matter does not play a significant role in this epoch, see also subsection 5.4, the energy density of matter is equal to the energy density of the baryons. This means that dark matter does not play any role in this plasma, in contrast to the Λ-CDM model where dark matter is a crucial component.

## 6.3 Equations of State

The equation of state, relating the pressure $p_i$ and the energy density $\rho_i$ of a substance $i$, can in general be written in a linear form as

$$p_i = \omega_i \rho_i, \tag{6.18}$$

where $\omega_i$ is a dimensionless number. For non-relativistic matter, $\omega_{\text{m}} = 0$, because the kinetic pressure is negligible relative to the mass. For radiation, $\omega_{\text{r}} = \frac{1}{3}$ [4]. From equations (5.5) and (5.6), it can be deduced that the vacuum energy density and pressure are given by

$$\rho_{\text{vac}} = C_{1/2} \left(-\frac{R}{6}\right)^{1/2}, \quad p_{\text{vac}} = -C_{1/2} \left(-\frac{R}{6}\right)^{1/2}, \tag{6.19}$$

i.e. $\omega_{\text{vac}} = -1$. The total pressure is simply the sum of all separate equations of state

$$P_{\text{tot}} = \sum_i p_i = \sum_i \omega_i \varepsilon_i = \frac{1}{3}\rho_{\text{r}} - C_{1/2} \left(-\frac{R}{6}\right)^{1/2}, \tag{6.20}$$

where we sum over $i$ = r, m, vac. It is important to note that only interacting fluid components can exert a pressure in the plasma. The interacting components are photons and baryons, as mentioned in subsection 6.2. This means that the total pressure on the fluid components is

$$P_{\text{fluid}} = \frac{1}{3}\rho_\gamma - C_{1/2} \left(-\frac{R}{6}\right)^{1/2}. \tag{6.21}$$

The Ricci scalar can be rewritten using both acceleration equations (5.4) and (5.10) as

$$-\frac{R}{6} = \left(\frac{\ddot{a}}{a} + \frac{\dot{a}^2}{a^2}\right) \tag{6.22}$$

$$= 2\frac{\ddot{a}}{a} + 4\pi G(\rho + p) \tag{6.23}$$

$$= \frac{4\pi G}{3}\left(\rho - 3p + 2\beta + 2\sqrt{\beta(\rho - 3p + \beta)}\right). \tag{6.24}$$

In the vacuum energy pressure term, the C$\nu$B (and negligible created matter) components still do play a role and cannot be omitted, so we still have $\rho_{\mathrm{r}}$ and $\rho_{\mathrm{m}}$ terms. By inserting $\rho = \rho_m + \rho_r$ and $p = p_m + p_r = \frac{1}{3}\rho_r$ in (6.24) we can find the total fluid pressure

$$P_{\mathrm{fluid}} = \frac{1}{3}\rho_\gamma - C_{1/2}\left(\frac{4\pi G}{3}\left(\rho_{\mathrm{m}} + 2\beta\left(1 + \sqrt{1 + \frac{\rho_{\mathrm{m}}}{\beta}}\right)\right)\right)^{1/2}. \tag{6.25}$$

This equation is only valid in the early universe, when the universe consisted of a baryon-photon fluid [16]. The radiation pressure and gravity set up oscillations in this fluid, called acoustic density waves. If only a single density perturbation in the plasma is considered, the wave will propagate outwards as an acoustic wave with the speed of sound (see the next subsection). After the moment of last scattering, photons can travel freely, propagating as a free stream of photons forming the cosmic microwave background. After the drag epoch, when the baryons are decoupled from the photons, the baryon wave stalls. This results in density fluctuations that are present on a comoving scale (this is a distance scale that is constant under the expansion of the universe), called baryonic acoustic oscillations. We will briefly discuss the drag epoch in subsection 6.8

## 6.4 Speed of Sound

In a photon-baryon fluid it is possible to have pressure waves, which are more intuitively referred to as sound waves, that could move through the photon-baryon fluid. The speed of sound squared [17, 18] is defined as

$$c_s^2 \equiv \left(\frac{\mathrm{d}P_{\mathrm{fluid}}}{\mathrm{d}\rho_{\mathrm{fluid}}}\right)_S, \tag{6.26}$$

where $\rho_{\mathrm{fluid}}$ is the energy density of the components in the fluid that can feel the pressure

$$\rho_{\mathrm{fluid}} = \rho_\gamma + \rho_{\mathrm{b}}. \tag{6.27}$$

The subscript $S$ refers to a constant entropy. We assume this to be the case, because the change in entropy due to the interactions of photons and baryons is accounted for by electron-photon Thomson scattering terms [17]. Furthermore, we can safely ignore matter creation in the early universe.
The speed of sound is not solvable for equation (6.25). In the photon-baryon fluid of the early universe, photons were the most dominant substance in terms of total pressure on the fluid components, so we can make the assumption that

$$P_{\mathrm{fluid}} \approx p_\gamma = \frac{1}{3}\rho_\gamma. \tag{6.28}$$

We can now calculate the speed of sound as

$$c_s^2 = \frac{\mathrm{d}P_{\mathrm{tot}}}{\mathrm{d}\rho_{\mathrm{fluid}}} \approx \frac{\mathrm{d}p_\gamma}{\mathrm{d}\rho_{\mathrm{fluid}}} = \frac{\mathrm{d}p_\gamma}{\mathrm{d}\rho_\gamma}\frac{\mathrm{d}\rho_\gamma}{\mathrm{d}\rho_{\mathrm{fluid}}} = \frac{\mathrm{d}p_\gamma}{\mathrm{d}\rho_\gamma}\left(\frac{\mathrm{d}\rho_{\mathrm{fluid}}}{\mathrm{d}\rho_\gamma}\right)^{-1} = \frac{1}{3}\left(1 + \frac{\partial\rho_{\mathrm{b}}}{\partial\rho_\gamma}\right)^{-1}. \tag{6.29}$$

It is helpful to rewrite this equation in terms of redshift $z$. This allows us to study the evolution of the speed of sound. Equation (6.29) then becomes

$$c_s^2 = \frac{1}{3}\left(1 + \frac{\partial \rho_\mathrm{b}}{\partial z}\left(\frac{\partial \rho_\gamma}{\partial z}\right)^{-1}\right)^{-1}. \tag{6.30}$$

We can substitute $\rho_\mathrm{b} = \rho_{\mathrm{b,ls}}\frac{(z+1)^3}{(z_\mathrm{ls}+1)^3}$ and $\rho_\gamma = \rho_{\gamma,\mathrm{ls}}\frac{(z+1)^4}{(z_\mathrm{ls}+1)^4}$ to get an equation dependent on only the energy densities. The subscript 'ls' denotes the moment of last scattering. The speed of sound in the photon-baryon plasma can then be expressed as

$$c_s^2 = \frac{1}{3}\left(1 + \frac{3}{4}\frac{\rho_\mathrm{b}}{\rho_\gamma}\right)^{-1}. \tag{6.31}$$

## 6.5 Sound Horizon

The maximum distance a sound wave could have travelled in the photon-baryon plasma before recombination is called the sound horizon. The sound horizon is seen as one of the standard candles in cosmology and is therefore an important quantity. The comoving length of the sound horizon, $r_\mathrm{s}$, is related to the proper distance of the sound horizon, $d_\mathrm{s}$, as

$$r_\mathrm{s} = d_\mathrm{s}(1 + z_\mathrm{ls}) = \int_0^{t_\mathrm{ls}} \frac{c_\mathrm{s}(t)}{a(t)}\mathrm{d}t \tag{6.32}$$

$$d_\mathrm{s} = a(t_\mathrm{ls})\int_0^{t_\mathrm{ls}} \frac{c_\mathrm{s}(t)}{a(t)}\mathrm{d}t, \tag{6.33}$$

where we have used that $a(t_\mathrm{ls}) = \frac{1}{1+z_\mathrm{ls}}$. The integral over time can be rewritten as an integral over redshift, which makes it easier to do calculations. The relation between redshift $z$ and the scale factor $a$ is given in (3.5), this can be rewritten to

$$z = \frac{1}{a} - 1. \tag{6.34}$$

Differentiating this equation with respect to time gives

$$\frac{\mathrm{d}z}{\mathrm{d}t} = \dot{z} = -\frac{1}{a^2}\dot{a} = -\frac{1}{a}H, \tag{6.35}$$

from which it follows that

$$-\frac{1}{H}\mathrm{d}z = \frac{1}{a}\mathrm{d}t. \tag{6.36}$$

A boundary condition of $t = 0$ corresponds to $z = \infty$ and $t = t_0$ corresponds to $z = 0$. The sound horizon can then be expressed as

$$r_\mathrm{s} = \int_{z_\mathrm{ls}}^{\infty} \frac{c_\mathrm{s}(z)}{H(z)}\mathrm{d}z. \tag{6.37}$$

## 6.6 Moment of Last Scattering

The CMB photons we can detect have been travelling as a free photon stream through the universe since the moment they last scattered off a free electron. The probability that a photon undergoes a scattering during a short time $t \to t + \mathrm{d}t$ is given by

$$\mathrm{d}P = \Gamma(t)\mathrm{d}t, \tag{6.38}$$

where $\Gamma(t)$ is the scattering rate at time $t$. For the physics behind $\Gamma(t)$, I would like to refer to Thijs van Rossum's thesis [3], where he spent a great deal of time implementing this quantity in his Python script, making it simple for us to use it for calculations. For a CMB photon measured at the present time $t_0$, the expected number of scatterings since an earlier time $t$ is

$$\tau(t) = \int_t^{t_0} \Gamma(t)\mathrm{d}t. \tag{6.39}$$

We can rewrite this equation in terms of the scale factor $a$ as

$$\tau(a) = \int_a^1 \Gamma(a)\frac{\mathrm{d}a}{\dot{a}} = \int_a^1 \frac{\Gamma(a)}{H(a)}\frac{\mathrm{d}a}{a}. \tag{6.40}$$

Following the same procedure as in subsection 6.5 we can also write this in terms of redshift $z$

$$\tau(z) = \int_0^z \frac{\Gamma(z)}{H(z)}\frac{1}{1+z}\mathrm{d}z \tag{6.41}$$

The moment of last scattering is defined as the moment when $\tau = 1$. This leaves us the following equation to solve the redshift value of last scattering

$$1 = \int_0^{z_{\mathrm{ls}}} \frac{\Gamma(z)}{H(z)}\frac{1}{1+z}\mathrm{d}z. \tag{6.42}$$

This gives us a value of $z_{\mathrm{ls}} = 1270$, according to the calculation in section 9.

## 6.7 Moment of Big Bang Nucleosynthesis

The infinity in the integral in (6.37) does not really represent true infinity, but rather the moment at which the sound wave could begin its journey. We assume this to be right after big bang nucleosynthesis (BBN). The sound horizon can thus be expressed as

$$r_{\mathrm{s}} = \int_{z_{\mathrm{ls}}}^{z_{\mathrm{nuc}}} \frac{c_{\mathrm{s}}(z)}{H(z)}\mathrm{d}z. \tag{6.43}$$

BBN occurred when the nuclei had a temperature of $T_{\mathrm{nuc}} = 7.6 \cdot 10^8$ K [4]. The universe was in thermal equilibrium in this epoch, since this is before last scattering. We also found that $T \propto a^{-1}$ in (6.6), so we can use the temperature of the CMB photons to calculate the corresponding redshift value as

$$T = T_0 a^{-1} = T_0(z+1) \quad \Rightarrow \quad z = \frac{T}{T_0} - 1 \quad \Rightarrow \quad z_{\mathrm{nuc}} = \frac{T_{\mathrm{nuc}}}{T_0} - 1, \tag{6.44}$$

where $T_0 = 2.7255 \pm 0.0006\,\mathrm{K}$ [12] is the present time temperature of the CMB photons. So the redshift value for BBN is

$$z_{\mathrm{nuc}} = \frac{7.6 \cdot 10^8}{2.7255} - 1 \approx 2.79 \cdot 10^8. \tag{6.45}$$

In reality the sound wave could even begin during (or before) BBN, but integrating up to $z_{\mathrm{nuc}}$ provides a very good approximation for the sound horizon. We will discuss this in section 9.4.

## 6.8 Drag Epoch

The ratio of the number densities of baryons and photons is constant over time since the baryons were formed. This so-called baryon-to-photon ratio [4] is $\eta = (6.10 \pm 0.06) \cdot 10^{-10}$.

Due to the much larger number density of photons, the moment of decoupling of photons from the baryons and the moment of decoupling of the baryons from the photons is not the same. Since there are less baryons than photons, the average photon does not feel the influence of the baryons from a certain moment. Meanwhile due to the much larger number of photons, the baryons still feel the influence of the photons. The moment the baryons are released from the drag of the photons is called the drag epoch (denoted with redshift $z_{\mathrm{d}}$) [19]. The moment the photons are decoupled from the baryons is called the moment of last scattering ($z_{\mathrm{ls}}$). The drag epoch happens at a later stage than the moment of last scattering, i.e. $z_{\mathrm{d}} < z_{\mathrm{ls}}$.
This results in two different calculations of the sound horizon, one for a sound wave travelling in the plasma until $z_{\mathrm{ls}}$, as calculated in equation (6.43), and one sound horizon as a result of a baryonic density fluctuation travelling until $z_{\mathrm{d}}$. In the $\Lambda$-CDM model this results in a small difference of the sound horizon [20], related by

$$r_{\mathrm{s}}(z_{\mathrm{d}}) = 1.0184 r_{\mathrm{s}}(z_{\mathrm{ls}}). \tag{6.46}$$

Our expectation is that in the CDDE model the two sound horizons also differ just slightly, since these calculations are based on pre-recombination physics, where dark energy is negligible.

# 7 Cosmic Microwave Background

The cosmic microwave background (CMB) is a faint, uniform glow of microwave radiation that radiates through the entire universe. It is an observable remnant of the photon-baryon fluid in the early universe, offering insights into the physics of this plasma. Its spectrum closely approximates that of a perfect black body, which allows us to determine its temperature. The mean present-day temperature across the sky is measured as $T_0 \equiv \langle T_0 \rangle = 2.7255 \pm 0.0006\,\mathrm{K}$ [12]. There are also tiny fluctuations (anisotropies) in the temperature, which are of the order of $10^{-4} - 10^{-5}\,\mathrm{K}$. These fluctuations are depicted in figure 6. The tiny fluctuations in temperature provide us with information about the distribution of energy in the photon-baryon fluid.

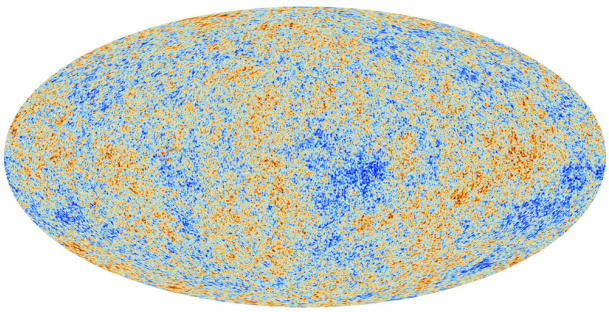

Figure 6: A heat map of the temperature fluctuations in the cosmic microwave background [21].

## 7.1 Power Spectrum

The temperature fluctuations can be expressed as density fluctuations $\delta T/T$, where we define $T \equiv \langle T \rangle$. The fluctuations can be seen as a function defined on the surface of a celestial sphere and can therefore be written as a sum of simpler components:

$$\frac{\delta T}{T}(\theta, \phi) \equiv \frac{T(\theta, \phi) - \langle T \rangle}{\langle T \rangle} = \sum_{l=0}^{\infty} \sum_{m=-l}^{l} a_{lm} Y_{lm}(\theta, \phi), \tag{7.1}$$

where $\langle T \rangle$ is the average temperature and $Y_{lm}$ are the spherical harmonics. This is comparable to how Fourier series decompose functions into sinusoidal components. The most important statistical property of $\delta T/T$ is the correlation function $C(\varphi)$. The correlation function quantifies how similar the temperature fluctuations are at different points on the celestial sphere at the moment of last scattering. The correlation function can be obtained by considering two points on the sphere, in the directions $\hat{n}(\theta, \phi)$ and $\hat{n}'(\theta', \phi')$ and separated by an angle $\varphi$ relative to an observer. The relation between $\varphi$, $\hat{n}$ and $\hat{n}'$ is $\cos\varphi = \hat{n} \cdot \hat{n}'$. The correlation function is then found by multiplying $\delta T/T$ at the two points and averaging the product over all points separated by the angle $\varphi$:

$$C(\varphi) = \left\langle \frac{\delta T}{T}(\hat{n}) \frac{\delta T}{T}(\hat{n}') \right\rangle_{\hat{n} \cdot \hat{n}' = \cos\varphi}. \tag{7.2}$$

By plugging in equation (7.1), the correlation function can be written in the form

$$C(\varphi) = \frac{1}{4\pi} \sum_{l=0}^{\infty} (2l+1) C_l P_l(\cos\varphi), \tag{7.3}$$

where $P_l(\cos\varphi)$ are the Legendre polynomials. The measured correlation function can now be broken down into its angular power spectrum $C_l = \langle |a_{lm}|^2 \rangle$. Since the statistical properties are independent on the choice of the origin (rotational invariance), the result cannot depend on the index $m$. The angular power spectrum is therefore only dependent on $l$. The index $l$, which is the multipole moment, can be thought of as the angular scale. As a rule of thumb, $C_l$ is telling us something about the anisotropies on an angular scale of [22]

$$\varphi = \frac{180^\circ}{l}. \tag{7.4}$$

The $l = 0$ (monopole) term vanishes if the mean temperature is correctly defined. The $l = 1$ (dipole) term is primarily a result of the Doppler shift due to the motion of the earth through space. The multipole moments with $l \geq 2$ tell us something about the temperature fluctuations at the moment of last scattering [4].

In presenting the CMB observations, it is a convention to plot $l(l+1)C_l/(2\pi) = \left(\frac{\Delta T}{T}\right)^2$ as a function of the multipole moment $l$. This plot is called the power spectrum and is depicted in figure 7. In power spectrum plots the dipole is always removed, since this is not interesting to study from a cosmological point of view.

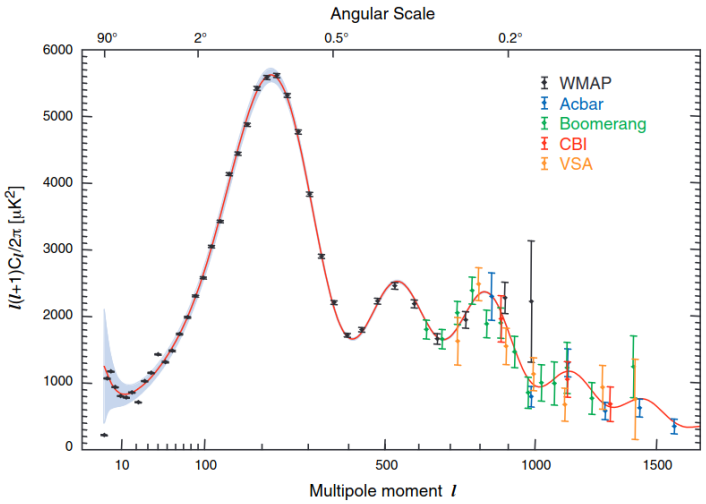


Figure 7: The power spectrum of the cosmic microwave background temperature anisotropies as a function of the multipole moment as measured by a variety of experiments [1]. Note that in this plot $C_l$ is defined using $\Delta T$ rather than $\frac{\Delta T}{T}$, therefore the y-axis is equal to $(\Delta T)^2$.

## 7.2 Multipole Moment of the First Peak

Since the multipole moment is related to the angular scale in equation (7.4), it is possible to calculate the multipole moment of the first peak in the power spectrum via

$$\theta_{\mathrm{A}} = \frac{180^\circ}{l_{\mathrm{A}}} = \frac{\pi\,(\text{radians})}{l_{\mathrm{A}}} \quad \Rightarrow \quad l_{\mathrm{A}} = \frac{\pi}{\theta_{\mathrm{A}}}. \tag{7.5}$$

The characteristic angle $\theta_{\mathrm{A}}$ is defined as [23]

$$\theta_{\mathrm{A}} \equiv \frac{r_{\mathrm{s}}(z_{\mathrm{ls}})}{d_{\mathrm{A}}(z_{\mathrm{ls}})}, \tag{7.6}$$

where $r_s$ is the sound horizon as in equation (6.37) and $d_A$ is the angular diameter distance. The angular diameter distance is a distance measure defined in terms of the objects physical size and its angular size as seen from Earth. In a spatially flat universe, the angular diameter distance is given by

$$d_A = \int_0^{z_{ls}} \frac{dz}{H(z)}. \tag{7.7}$$

Combining equations (6.37), (7.5), (7.6) and (7.7) makes it possible to calculate the multipole moment as

$$l_A = \pi \int_0^{z_{ls}} \frac{dz}{H(z)} \left( \int_{z_{ls}}^{\infty} \frac{c_s(z')}{H(z')} dz' \right)^{-1}. \tag{7.8}$$

## 7.3 Shift on the Multipole Moment

The multipole moment as given in (7.8) will not correspond to the multipole moment of the first peak in the power spectrum. This is a result of driving effects, such as the Doppler shift due to the oscillating fluid as well as the decay of the gravitational potential. The latter implies that baryonic matter is pulled towards regions of higher baryonic density, due to the gravitational pull. The gravitational potential is therefore converted into kinetic energy. This leads to a decay of the gravitational potential in lower density regions. Higher density regions become more bound. Both driving effects strengthen the oscillations and result in an increase in power [24]. This results in a phase shift. Investigating the numerical shift of the CMB power spectrum peaks is a complicated study in its own right and falls outside the scope of this thesis, but other papers investigating the shift can be found. One of the papers [25] presenting a general formula for the shift gives for the multipole moment of the first peak

$$l_1 = l_A(1 - \chi). \tag{7.9}$$

Here the shift $\chi$ is given by

$$\chi = (1.466 - 0.466 n_s) \left[ a_1 r_{ls}^{a_2} + 0.291 \bar{\Omega}_{ls}^{\phi} \right] \tag{7.10}$$

$$a_1 = 0.286 + 0.626 \Omega_{b,0} h^2 \tag{7.11}$$

$$a_2 = 0.1786 - 6.308 \Omega_{b,0} h^2 + 174.9 \left( \Omega_{b,0} h^2 \right)^2 - 1168 \left( \Omega_{b,0} h^2 \right)^3 \tag{7.12}$$

$$r_{ls} = \frac{\rho_r(z_{ls})}{\rho_m(z_{ls})} = \frac{\Omega_r(z_{ls})}{\Omega_m(z_{ls})} \tag{7.13}$$

$$h = h_0 = \frac{H_0^{late}}{100\,\mathrm{km\,s^{-1}\,Mpc^{-1}}} \tag{7.14}$$

$$\bar{\Omega}_{ls}^{\phi} = t_{ls}^{-1} \int_0^{t_{ls}} \Omega^{\phi}(t) dt. \tag{7.15}$$

During this epoch, $\rho_m \approx \rho_b$. The variable $n_s$ is the scalar spectral index. The scalar spectral index describes whether the density fluctuations in the plasma are spatial scale invariant. A value of $n_s = 1$ corresponds to spatial scale invariance. The value of the scalar spectral index is a result of inflationary models [26]. The Planck Collaboration [27] found $n_s = 0.965 \pm 0.004$. According to the Planck Collaboration, this result is weakly dependent on the Λ-CDM model and it remains stable, with slightly increased errors, when considered in most other extensions. Therefore, we will use $n_s = 0.965$ in the CDDE model and leave it to future research to show if this is indeed the correct value in this model (see section 10).

The notation for $\bar{\Omega}_{\text{ls}}^{\phi}$ is taken from [28] and is the average dimensionless quintessence energy fraction before last scattering, i.e. for $z > z_{\text{ls}}$. The quintessence component represents a dark energy that changes over time, just like in our model. Here the assumption is made that the fraction of quintessence energy does not change rapidly before last scattering, which is the case in our CDDE model. Formula (7.10) is obtained using a standard exponential potential for the quintessence component. The writers of the paper expect the results to be approximately correct for any realization of quintessence. For example, this formula is also applied (in a more simplified form) in the $\Lambda(t)$-CDM model, where the cosmological 'constant' $\Lambda$ is dependent on time [29].

# 8 Baryonic Acoustic Oscillations

## 8.1 Correlation Function

The baryonic density fluctuations present in the photon-baryon plasma are called baryonic acoustic oscillations (BAO). After the drag epoch, the baryon overdensities were small in amplitude. These low-amplitude fluctuations grew to detectable levels at the present time (but still small enough to not undermine the assumption that the universe is homogeneous and isotropic). The best way to detect these overdensities on large scales is to look at the correlation function $\xi$ of galaxies. Assume the number density of galaxies at the present day to be $n_{\text{gal}}$. Pick a random galaxy, then look at a small volume $\mathrm{d}V$ at a comoving distance $r$ around that galaxy. The correlation function then tells you how many other galaxies you would expect to find in this volume [4]. As a mathematical equation this can be expressed as

$$\mathrm{d}N = n_{\text{gal}} \left[1 + \xi(r)\right] \mathrm{d}V. \tag{8.1}$$

If the galaxies would follow a Poisson distribution, the correlation function would vanish. It turns out galaxies do not follow a Poisson distribution. Due to gravitational effects, you would expect galaxies to attract each other, leading to the clustering of galaxies. The correlation function of galaxies $\xi$ as a function of the comoving separation $s$ is depicted in figure 8. This comoving separation is determined by measuring the redshift of galaxies [30, 31], which is related to the comoving separation by the formula

$$z = H_0 s, \tag{8.2}$$

where $z$ is the redshift, $H_0$ is the Hubble constant and $s$ is the comoving separation [4]. We will use $H_0^{\text{late}}$ as defined in subsection 4.1 to derive $s$, since this is assumed to be cosmological model independent. It is a convention to use $h$ as a parameter for the Hubble constant, $h$ is defined as $h \equiv \frac{H_0}{100\,\mathrm{km\,s^{-1}\,Mpc^{-1}}} = 0.733$.

## 8.2 BAO Bump

Around a comoving separation of $s_{\text{bump}} = 105\mathrm{h}^{-1}\,\mathrm{Mpc} = 143\,\mathrm{Mpc}$, there is a bump in the correlation function. This BAO bump is due to the sound waves present in the photon-baryon fluid and corresponds to the sound horizon calculated at the drag epoch $z_{\mathrm{d}}$ [16]. This gives us as a measured value of $s_{\text{bump}} = r_{\mathrm{s}}(z_{\mathrm{d}}) = 143\,\mathrm{Mpc}$.
We will not discuss the BAOs in any more depth, since this thesis focusses on the CMB. Nevertheless, the BAO bump provides us with a rough approximation for what we should expect for the sound horizon at the moment of last scattering. The two sound horizons should only differ by a small factor, as discussed in subsection 6.8. This results in an expected value for the sound horizon at last scattering of

$$r_{\mathrm{s}}(z_{\mathrm{ls}}) \approx \frac{r_{\mathrm{s}}(z_{\mathrm{d}})}{1.0184} = \frac{143\,\mathrm{Mpc}}{1.0184} = 141\,\mathrm{Mpc}. \tag{8.3}$$

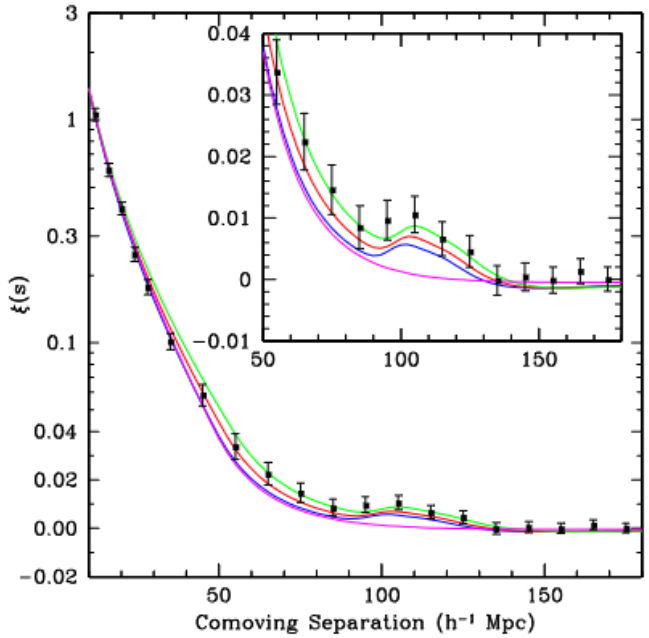


Figure 8: Correlation function of galaxies $\xi$ plotted against the comoving separation s [30]. The BAO bump is clearly visible at $s_{\text{bump}} = 105\text{h}^{-1}\,\text{Mpc}$, where $h = \frac{H_0^{\text{late}}}{100\,\text{km}\,\text{s}^{-1}\,\text{Mpc}^{-1}} = 0.733$. This results in a comoving separation $s_{\text{bump}} = 143\,\text{Mpc}$.

# 9 Numerical Results

## 9.1 Dimensionless Density Parameters and Hubble Parameter

Using the Python script Thijs van Rossum wrote for his master thesis [3], we can generate a variety of variables for a range of redshift values [3]. We can extract values for $H$, $\Omega_{\mathrm{r}}$, $\Omega_{\mathrm{m}}$, $\Omega_\beta$ and $\Gamma(t)$. All the additional code required to do the calculations is provided in appendix A. This code should be added on top of Thijs van Rossum's script. The moment of last scattering can be calculated using equation (6.42), which results in $z_{\mathrm{ls}} = 1270$. This allows us to make plots of the evolution of the dimensionless density parameters $\Omega_i$ and the Hubble parameter $H$. These plots are depicted in figures 9, 10 and 11.

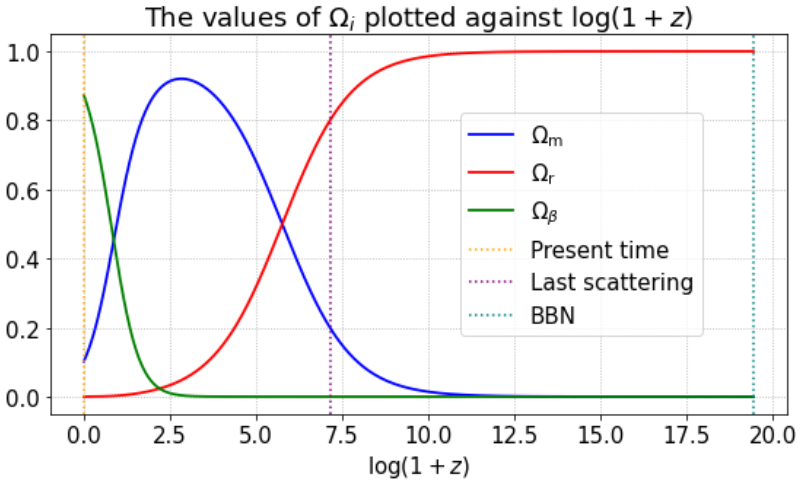


Figure 9: The evolution of the dimensionless density parameters $\Omega_i$ during the plasma phase up to the present time. This graph shows that radiation was the most dominant substance during the plasma phase.

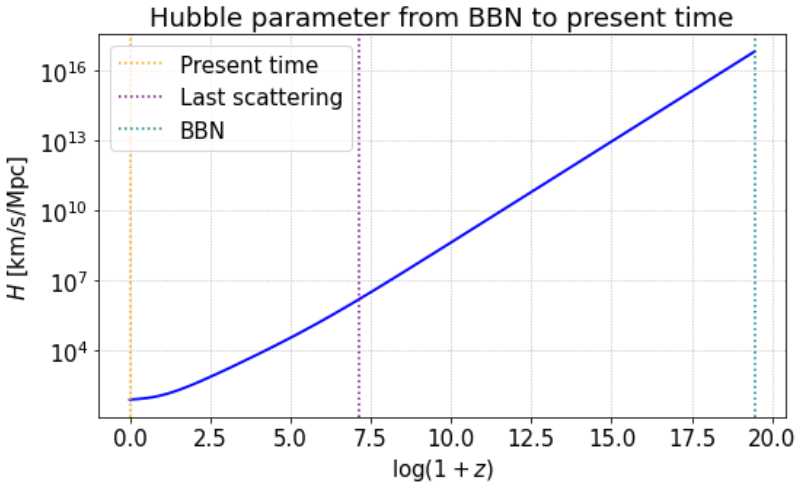


Figure 10: The evolution of the Hubble parameter $H$ during the plasma phase up to the present time. The Hubble parameter increases rapidly for high redshift values.

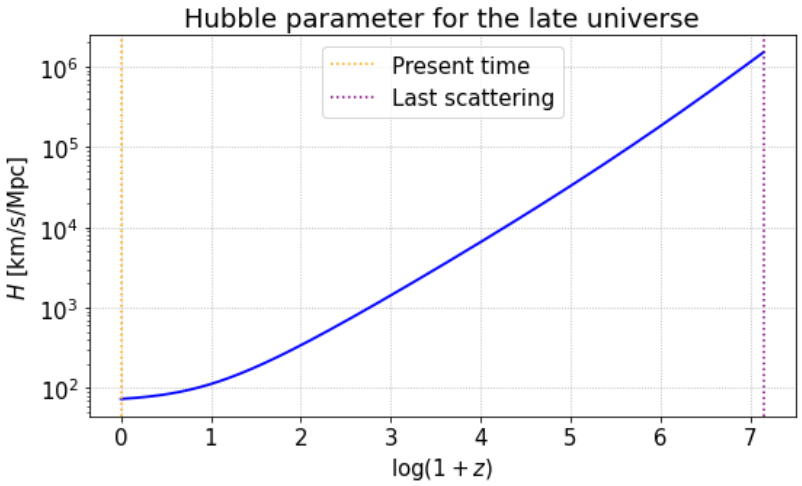


Figure 11: The evolution of the Hubble parameter $H$ during the late universe. This plot shows that the Hubble parameter also grows rapidly during the late universe epoch.

In figure 9, we can see that radiation-matter equality occurred around $\log(1+z) \approx 6$. In the $\Lambda$-CDM model, this equality occurred at $\log(1+z) \approx 8$, which is even earlier than the moment of last scattering (in $\Lambda$-CDM, $\log(1+z_{\text{ls}}) = 7$) [4]. This difference is due to the larger dark matter component in $\Lambda$-CDM, making the non-relativistic matter component more significant during an earlier stage.
Matter-dark energy equality happened around $\log(1+z) \approx 1$. In the $\Lambda$-CDM model, this occurred around $\log(1+z) \approx 0.3$. Therefore, in the CDDE model dark energy becomes more important at an earlier moment and, subsequently, matter becomes less important at an earlier stage when compared to the $\Lambda$-CDM model. This is due to the smaller (dark) matter component in CDDE compared to the $\Lambda$-CDM model.
In the near future, the universe will be completely dark energy dominated, i.e. equation (5.14) will become $\Omega_\beta = 1$, where $\Omega_\beta = \frac{8\pi G}{3H^2}\beta$. This results in a constant Hubble parameter. If we examine the Ricci scalar in equation (6.24) and we set the matter and radiation energy densities to zero, we can deduce that $\left(-\frac{R}{6}\right)^{1/2}$ becomes a constant. The vacuum energy density in equation (6.19) also becomes constant, specifically:

$$\rho_{\text{vac}} = C_{1/2}\sqrt{\frac{16\pi G}{3}}\beta. \tag{9.1}$$

In the future, our CDDE model will behave like a model with a cosmological constant.

## 9.2 Speed of Sound

Now that we have the $\Omega_i$-values for radiation (and therefore for the CMB photons, see equation (6.15)) and matter, we can calculate $\Omega_{\text{b},0}$ using that according to our model $\Omega_{\text{b}} = \Omega_{\text{m}}$ for high values of redshift, such as $z_{\text{ls}}$. Since baryons still evolve as $\rho_{\text{b}} \propto a^{-3}$, we can rewrite equation (5.20) and calculate $\Omega_{\text{b},0}$ as follows:

$$\Omega_{\text{b},0} = \Omega_{\text{b,ls}}a_{\text{ls}}^3 = \Omega_{\text{m,ls}}a_{\text{ls}}^3 = \Omega_{\text{m,ls}}(1+z_{\text{ls}})^{-3}. \tag{9.2}$$

In this equation we replaced $\Omega_{\text{b,ls}}$ by $\Omega_{\text{m,ls}}$ in order to numerically calculate $\Omega_{\text{b},0}$. It is now possible to calculate the speed of sound in the photon-baryon fluid. The speed of sound is approximately $c_{\text{s}} \approx 1.73 \cdot 10^8$ m/s, see also figure 12.

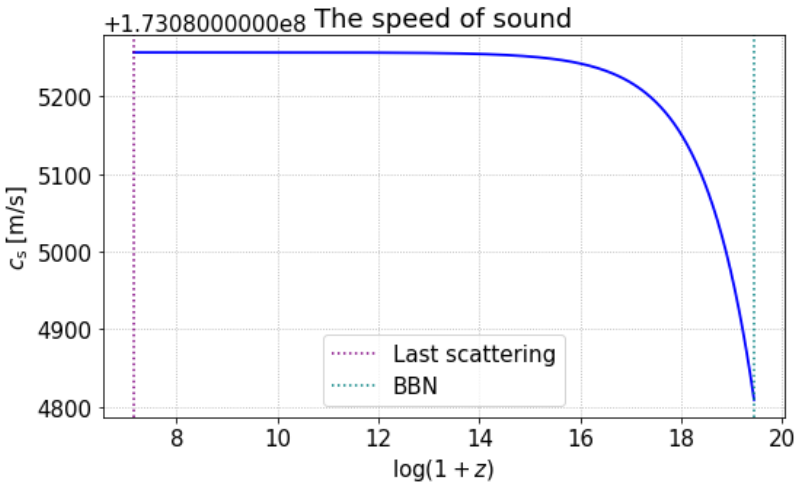


Figure 12: The speed of sound in the photon-baryon fluid epoch. Please note that the $y$-axis should be shifted by $1.7308 \cdot 10^8$. The graph then clearly shows that the speed of sound is nearly constant during most of the fluid phase.

## 9.3 Sound Horizon and Multipole Moment

The sound horizon is $r_s = 153\,\text{Mpc}$, where $r_{s,\text{expected}} \approx 141\,\text{Mpc}$ is expected (see section 8).
We can also calculate the theoretical multipole moment of the first peak with equation (7.8). This gives us $l_A = 513$. The phase shift can be implemented, such that the corrected first peak can be calculated, which is found to be $l_1 = 322$. In figure 7 we can see that the measured value is $l_{1,\text{measured}} \approx 220$.
These is a significant mismatch between the predictions in the CDDE model and the measured values, although they are in the correct ballpark. Therefore, a universe with as only dark matter source the creation of matter due to the curvature dependent dark energy is not viable.

## 9.4 Convergence of the Sound Horizon

We have already noted that integrating the sound horizon up to $z_{\text{nuc}}$ is not perfectly accurate. However, it does provide a good approximation because the sound horizon is converging for high $z$-values. This convergence can be observed in the following:
For high $z$-values the universe is radiation-dominated, and the Hubble parameter can be approximated as the Hubble parameter for a one-component universe [4]

$$H(z) \approx \text{constant} \cdot \sqrt{(z+1)^4} = \alpha(z+1)^2. \tag{9.3}$$

The sound horizon is almost constant and can be approximated as $c_s(z) \approx \text{constant} = c_s$.

The difference between two sound horizons with integrations up to $z_1$ and $z_2$ is as follows:

$$\int_{z_{\mathrm{ls}}}^{z_1} \frac{c_{\mathrm{s}}(z)}{H(z)}\mathrm{d}z - \int_{z_{\mathrm{ls}}}^{z_2} \frac{c_{\mathrm{s}}(z)}{H(z)}\mathrm{d}z = \int_{z_2}^{z_1} \frac{c_{\mathrm{s}}(z)}{H(z)}\mathrm{d}z \tag{9.4}$$

$$\approx \int_{z_2}^{z_1} \frac{c_{\mathrm{s}}}{\alpha(z+1)^2}\mathrm{d}z \tag{9.5}$$

$$\approx \frac{c_{\mathrm{s}}}{\alpha}\left(\frac{1}{z_2} - \frac{1}{z_1}\right) \tag{9.6}$$

$$\approx 0 \quad \text{for large } z_1, z_2. \tag{9.7}$$

Therefore, $H(z)$ increases faster than $z$ and, consequently, faster than the domain of integration.
The convergence can be numerically demonstrated by comparing the sound horizon integrated up to $z_{\mathrm{nuc}} = 2.79 \cdot 10^8$ with the sound horizon integrated up to $z = 10^5$. This difference in the integration range results in a change in the sound horizon of $\Delta r_{\mathrm{s}} = 0.8$. As a consequence, the difference in multipole moment of the first peak is $\Delta l_1 = 1.5$.

# 10 Conclusion and Outlook

Our predictions do not match the expected values for the sound horizon and the location of the first peak in the power spectrum, but they are in the correct ballpark, so the CDDE model is not completely dead (yet). This means that a universe with a creation of dark matter due to the curvature dependent dark energy as the only dark matter source is not feasible. This model can be tweaked to include other sources as well, this can be done by implementing a third non-relativistic matter component in equation (6.17):

$$\rho_{\mathrm{m}} = \rho_{\mathrm{b}} + \rho_{\mathrm{created}} + \rho_{\mathrm{dark,other}}. \tag{10.1}$$

By creating another parameter one could investigate the necessary energy density of this third term to get the correct sound horizon and multipole moment.
Other studies can focus on determining the redshift value of the drag epoch within the CDDE model, allowing for a more accurate comparison of the sound horizon at $z_{\mathrm{d}}$ and the BAO peak.
To obtain a more accurate calculation for the sound horizon, one should also consider the physics during BBN and before. This is a challenge to implement in the equations because during BBN the mixture of the plasma was changing due to the creation of elements heavier than hydrogen through fusion. Furthermore, the transition of non-relativistic matter to relativistic matter in the very early universe adds another layer of complexity, since the dark energy density explicitly depends on the amount of non-relativistic matter.
One could also focus on the physics of the shift of the multipole moment, and implement this specifically for the CDDE model. You can even calculate the entire CMB power spectrum for the CDDE model. Using already available software, such as CAMB or CMBFAST, is not viable for models that differ a lot from Λ-CDM, because the software is written for constant dark energy models and would need a lot of modification for dynamical dark energy models. Writing your own program makes this easier to do. One paper that shows a self-contained description on how to do this is [32]. To do this accurately, one should investigate the physics of the scalar spectral index, as described in 7.3
Our fellow student Jesse Cools will focus on the cosmic neutrino background in the CDDE model. He will investigate the physics involved in the creation of this background and potential distortions caused by the matter creation effect within the CDDE model.

# 11 References


[1] G. Hinshaw, M. R. Nolta, C. L. Bennett, R. Bean, O. Dore, M. R. Greason, M. Halpern, R. S. Hill, N. Jarosik, A. Kogut, E. Komatsu, M. Limon, N. Odegard, S. S. Meyer, L. Page, H. V. Peiris, D. N. Spergel, G. S. Tucker, L. Verde, J. L. Weiland, E. Wollack, and E. L. Wright. Three-year wilkinson microwave anisotropy probe (wmap) observations: Temperature analysis. *The Astrophysical Journal Supplement Series*, 170(2):288–334, jun 2007.

[2] Bas van den Hoek. A curvature-dependent dark energy and how it can solve the hubble tension. Bachelor's thesis, Radboud University, July 2023. `https://www.ru.nl/publish/pages/913454/bas_van_den_hoek_bachelorscriptie.pdf`.

[3] Thijs van Rossum. Solving the hubble tension with a curvature dependent dark energy. Master's thesis, University of Twente, October 2023.

[4] Barbara Ryden. *Introduction to Cosmology*. Cambridge University Press, 2nd edition, 2017.

[5] Pavan Kumar Aluri, Paolo Cea, Pravabati Chingangbam, Ming-Chung Chu, Roger G Clowes, Damien Hutsemékers, Joby P Kochappan, Alexia M Lopez, Lang Liu, Niels C M Martens, C J A P Martins, Konstantinos Migkas, Eoin Ó Colgáin, Pratyush Pranav, Lior Shamir, Ashok K Singal, M M Sheikh-Jabbari, Jenny Wagner, Shao-Jiang Wang, David L Wiltshire, Shek Yeung, Lu Yin, and Wen Zhao. Is the observable universe consistent with the cosmological principle? *Classical and Quantum Gravity*, 40(9):094001, apr 2023.

[6] NASA. Geometry of the universe. `https://wmap.gsfc.nasa.gov/media/990006/index.html`, 2011. Accessed: 15-07-2023.

[7] Licia Verde, Tommaso Treu, and Adam G. Riess. Tensions between the early and late universe. *Nature Astronomy*, 3(10):891–895, sep 2019.

[8] AURA Astronomy. Our mysterious universe still evades cosmological understanding. `https://www.aura-astronomy.org/blog/2023/03/06/our-mysterious-universe-still-evades-cosmological-understanding/`, 2023. Accessed: 01-11-2023.

[9] Wim Beenakker and David Venhoek. A structured analysis of Hubble tension. `https://arxiv.org/abs/2101.01372`, 2021.

[10] Adam G. Riess, Alexei V. Filippenko, Peter Challis, Alejandro Clocchiatti, Alan Diercks, Peter M. Garnavich, Ron L. Gilliland, Craig J. Hogan, Saurabh Jha, Robert P. Kirshner, B. Leibundgut, M. M. Phillips, David Reiss, Brian P. Schmidt, Robert A. Schommer, R. Chris Smith, J. Spyromilio, Christopher Stubbs, Nicholas B. Suntzeff, and John Tonry. Observational evidence from supernovae for an accelerating universe and a cosmological constant. *The Astronomical Journal*, 116(3):1009–1038, sep 1998.

[11] Viatcheslav Mukhanov. *Physical Foundations of Cosmology*. Cambridge University Press, 1st edition, 2005.

[12] R. L. Workman *et al.* (Particle Data Group). Review of Particle Physics. *PTEP*, 2022:083C01, 2022.

[13] Rodney Loudon. *The Quantum Theory of Light*. Oxford Science Publications, 3th edition, 2000.

[14] Duvan Ricardo Herrera Herrera. *Spherical Collapse Model and Cosmic Acceleration*. PhD thesis, Universidade Federal Do Rio De Janeiro, April 2019.

[15] Bradley W. Carroll Dale A. Ostlie. *An Introduction to Modern Astrophysics*. Pearson, 2nd edition, 2021.

[16] Bruce A. Bassett and Renée Hlozek. Baryon Acoustic Oscillations. `https://arxiv.org/abs/0910.5224`, 2009.

[17] Chung-Pei Ma and Edmund Bertschinger. Cosmological perturbation theory in the synchronous and conformal newtonian gauges. *The Astrophysical Journal*, 455:7, dec 1995.

[18] P.J.E. Peebles. *Principles of Physical Cosmology*. Princeton University Press, 1st edition, 1993.

[19] Andoni Aizpuru, Rubén Arjona, and Savvas Nesseris. Machine learning improved fits of the sound horizon at the baryon drag epoch. *Physical Review D*, 104(4), aug 2021.

[20] Karsten Jedamzik, Levon Pogosian, and Gong-Bo Zhao. Why reducing the cosmic sound horizon alone can not fully resolve the Hubble tension. *Communications Physics*, 4(1), jun 2021.

[21] Chris North. Cosmic microwave background. `https://plancksatellite.org.uk/results/cosmic-microwave-background/`, 2013. Accessed: 28-08-2023.

[22] Andrew Liddle. *An Introduction to Modern Cosmology*. Wiley, 3th edition, 2015.

[23] Luca Amendola and Shinji Tsujikawa. *Dark Energy. Theory and Observations*. Cambridge University Press, 1st edition, 2010.

[24] Wayne Hu, Masataka Fukugita, Matias Zaldarriaga, and Max Tegmark. Cosmic microwave background observables and their cosmological implications. *The Astrophysical Journal*, 549(2):669–680, mar 2001.

[25] Michael Doran and Matthew Lilley. The location of cosmic microwave background peaks in a universe with dark energy. *Monthly Notices of the Royal Astronomical Society*, 330(4):965–970, mar 2002.

[26] Andrew Liddle and David Lyth. *Cosmological Inflation and Large-Scale Structure*. Cambridge University Press, 1st edition, 2000.

[27] Planck Collaboration. Planck 2018 results. VI. Cosmological parameters. *Astronomy & Astrophysics*, 641:A6, sep 2020.

[28] Michael Doran, Matthew Lilley, Jan Schwindt, and Christof Wetterich. Quintessence and the separation of cosmic microwave background peaks. *The Astrophysical Journal*, 559(2):501–506, oct 2001.

[29] C Pigozzo, M.A Dantas, S Carneiro, and J.S Alcaniz. Observational tests for $\Lambda(t)$CDM cosmology. *Journal of Cosmology and Astroparticle Physics*, 2011(08):022–022, aug 2011.

[30] Daniel J. Eisenstein *et al.* Detection of the baryon acoustic peak in the large-scale correlation function of sdss luminous red galaxies. *The Astrophysical Journey*, 633(2):560, nov 2005.

[31] Donald G. York *et al.* The sloan digital sky survey: Technical summary. *The Astronomical Journal*, 120(3):1579–1587, sep 2000.

[32] Petter Callin. How to calculate the cmb spectrum. https://arxiv.org/abs/astro-ph/0606683, 2006.

# A Python Code

Please note that the code should be incorporated into the code written by Thijs van Rossum [3].

```
# Importing libraries
import numpy as np
import matplotlib.pyplot as plt
from scipy import integrate
from scipy import constants

# Constants and u-values ---> u = log(1+z)
u = Sol.t

h = 0.733
H0 = 73.3 # km/s/Mpc
H0p = H0 * 10**3 # m/s/Mpc
H0s = H0p / (constants.mega*constants.parsec) # m/s/m = s^-1

H = H0p * np.exp(Sol.y[0]) # m/s/Mpc --> all H values, same index as u

# Calculating z_ls
index_for_present_time = np.argmin((u_array)**2)
u_array_past_time = u_array[index_for_present_time:]
Gamma_H_past_time = taudot_array[index_for_present_time:]

tau = np.array([])
for ii in range(len(u_array_past_time)):
    tau = np.append(tau, integrate.simpson(y = Gamma_H_past_time[:ii+1], x
                                           = u_array_past_time[:ii+1]))
u_ls = u_array_past_time[np.argmin((tau - 1)**2)]
z_ls = np.exp(u_ls) - 1

# Calculating Omega R/M at moment of last scattering
OmegaRls = Sol.y[2][np.argmin((np.exp(Sol.t)-1-z_ls)**2)]
OmegaMls = Sol.y[1][np.argmin((np.exp(Sol.t)-1-z_ls)**2)]

# Calculating the sound horizon at the moment of z_ls
def speed_of_sound(u):
    ''' Function to calculate the speed of sound as function of u, u
                                           should be larger than u_ls
        Dimension = [m/s]
    '''
    return constants.c/np.sqrt(3) * ( 1 + 3/4 * constants.c*3*H0s**2/(8*np
                                           .pi*constants.G) * OmegaM0/(4*
                                           constants.sigma*T0**4 * 1/(np.exp
                                           (u))))**(-1/2)

def integral_sound_horizon(u_ls):
    ''' Function provides the sound horizon for given u_value,integrates
                                           for u_ls to inf
    '''
    index_u = np.argmin((np.exp(Sol.t)-np.exp(u_ls))**2) # Finds index
                                           number corresponding with given u
                                           -value
    integrand = speed_of_sound(u[index_u:])/H[index_u:]*np.exp(u[index_u:]
                                           )
    return integrate.simpson(y = integrand, x = u[index_u:])

def integrand_hubble(u_ls):
    ''' Function to integrate 1/H*e^u du from 0 to u_ls
    '''
    index_u = np.argmin((np.exp(Sol.t)-np.exp(u_ls))**2) # Finds index
                                           number corresponding with given u
                                           -value
```

```
    integrand = np.exp(u[:index_u])/H[:index_u]
    return integrate.simpson(y = integrand, x = u[:index_u])

# Calculate sound horizon
sound_horizon = integral_sound_horizon(np.log(1 + z_ls)) # Sound horizon [
                                        Mpc]

# Calculate lA
l_A = constants.c * np.pi * integrand_hubble(np.log(1 + z_ls)) /
                                        sound_horizon

# Calculating the shift
omega_b_0 = OmegaMls * (z_ls + 1)**(-3)
r_ls = OmegaRls / OmegaMls # radiation-to-matter ratio at last scattering
omega_b_h = omega_b_0 * h**2
a1 = 0.286 + 0.626*omega_b_h
a2 = 0.1786 - 6.308*omega_b_h + 174.9*omega_b_h**2 - 1168*omega_b_h**3

# Calculating Omega_bar_phi
index_ls = np.argmin((np.exp(Sol.t)-1-z_ls)**2)
Omega_phi = Omega_beta_z[index_ls:]
u_values_phi = u[index_ls:]

Omega_bar_phi = 1/(np.log(1 + z_max) - np.log(1 + z_ls)) * integrate.
                                        simpson(y = Omega_phi, x =
                                        u_values_phi)

# Calculating l1
n_s = 0.965
phi =  (1.466 - 0.466*n_s)*( a1*r_ls**a2  +  0.291*Omega_bar_phi)
l1 = l_A * ( 1 - phi )
```